How to cite: Angew. Chem. Int. Ed. 2024, e202403493
doi.org/10.1002/anie.202403493

Biocatalysis

Insights into *E. coli* Cyclopropane Fatty Acid Synthase (CFAS) Towards Enantioselective Carbene Free Biocatalytic Cyclopropanation.

Iman Omar, Michele Crotti, Chuhan Li, Krisztina Pisak, Blazej Czemerys, Salvatore Ferla, Aster van Noord, Caroline E. Paul, Kersti Karu, Cagakan Ozbalci, Ulrike Eggert, Richard Lloyd, Sarah M. Barry, and Daniele Castagnolo**

Abstract: Cyclopropane fatty acid synthases (CFAS) are a class of *S*-adenosylmethionine (SAM) dependent methyltransferase enzymes able to catalyse the cyclopropanation of unsaturated phospholipids. Since CFAS enzymes employ SAM as a methylene source to cyclopropanate alkene substrates, they have the potential to be mild and more sustainable biocatalysts for cyclopropanation transformations than current carbene-based approaches. This work describes the characterisation of *E. coli* CFAS (*ec*CFAS) and its exploitation in the stereoselective biocatalytic synthesis of cyclopropyl lipids. *ec*CFAS was found to convert phosphatidylglycerol (PG) to methyl dihydrosterculate **1** with up to 58 % conversion and 73 % ee and the absolute configuration (9S,10R) was established. Substrate tolerance of *ec*CFAS was found to be correlated with the electronic properties of phospholipid headgroups and for the first time *ec*CFAS was found to catalyse cyclopropanation of both phospholipid chains to form dicyclopropanated products. In addition, mutagenesis and *in silico* experiments were carried out to identify the enzyme residues with key roles in catalysis and to provide structural insights into the lipid substrate preference of *ec*CFAS. Finally, the biocatalytic synthesis of methyl dihydrosterculate **1** and its deuterated analogue was also accomplished combining recombinant *ec*CFAS with the SAM regenerating *At*HMT enzyme in the presence of CH_3I and CD_3I respectively.

Introduction

The cyclopropane ring is a highly strained structural element found widely in natural products like terpenoids,[1] fatty acids[2] and in pharmaceuticals, including the drugs losmapimod,[3] tranylcypromine[4] and GSK1360707F (Figure 1).[5] The success of the cyclopropane ring in medicinal chemistry is due to its unique physiochemical properties resulting from its ring and torsional strain that confer high metabolic stability, conformational rigidity and lower lipophilicity than the corresponding non-cyclic isopropyl functional group.[6] The cyclopropyl ring is also a useful intermediate functionality in synthesis, as it can be opened using a variety of chemical methods.[7] Several synthetic approaches to access cyclopropanes as racemates or in enantiomerically pure form have been developed to date,[8] including, among the most important, the Simmons–Smith[9] and Corey–Chaykovsky[10] reactions. Although widely used in academia, current cyclopropanation methodologies have significant limitations in industry, as they require harsh reaction conditions, the use of stoichiometric metals, strong bases (NaH or BuLi), chiral auxiliaries and potentially explosive hazardous diazo-compound reagents.

In 2013, the research group of Frances Arnold pioneered the development of an enzymatic cyclopropanation reaction by engineering variants of cytochrome P450-BM3 to pro-

[*] I. Omar, Dr. M. Crotti, C. Li, K. Pisak, B. Czemerys, Dr. K. Karu, Dr. D. Castagnolo
Department of Chemistry, University College London
20 Gordon Street, WC1H 0AJ, London, United Kingdom
E-mail: d.castagnolo@ucl.ac.uk

I. Omar, Dr. M. Crotti, B. Czemerys, C. Ozbalci, Prof. U. Eggert, Dr. S. M. Barry
Department of Chemistry, Faculty of Natural, Mathematical and Engineering Sciences, King's College London
7 Trinity Street, SE1 1DB, London, United Kingdom
E-mail: sarah.barry@kcl.ac.uk

Dr. S. Ferla
Medical School, Faculty of Medicine, Health and Life Science, Swansea University
Swansea SA2 8PP

A. van Noord, Dr. C. E. Paul
Department of Biotechnology, Delft University of Technology
Van der Maasweg 9, 2629HZ Delft, The Netherlands

C. Ozbalci, Prof. U. Eggert
Randall Centre for Cell and Molecular Biophysics, Faculty of Life Sciences and Medicine, King's College London
London SE1 1UL, United Kingdom

Dr. R. Lloyd
DSD Chemistry, GSK Medicines Research Centre, Gunnels Wood Road, Stevenage, SG1 2NY

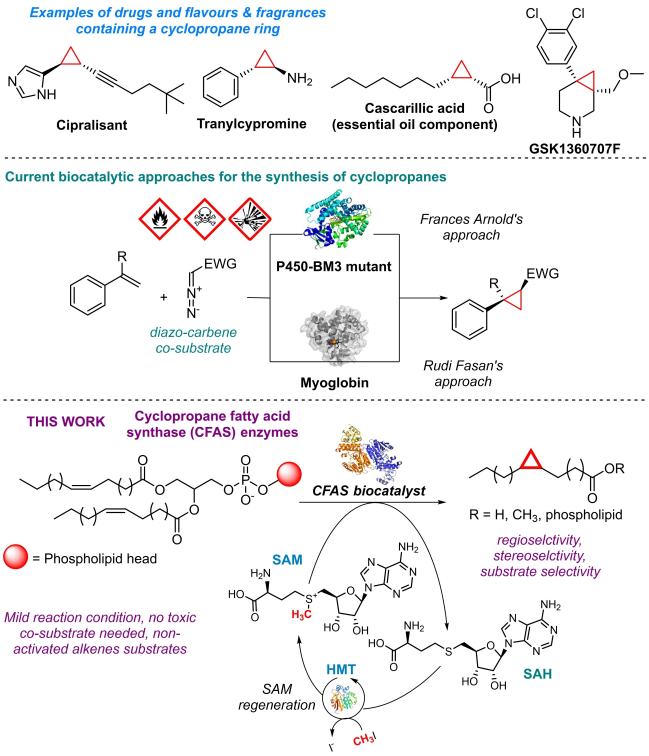

Figure 1. Current biocatalytic cyclopropanation methodologies and aim of this work.

duce new biocatalysts to promote the cyclopropanation of styrenes with good stereoselectivity and yields.[11] Later, Fasan's group reported the use of engineered myoglobin (MbH64V, V68A) for highly selective cyclopropanation reactions (Figure 1),[12] while Balskus used a biocompatible iron(III) phthalocyanine catalyst for the cyclopropanation of styrene.[13]

While these novel biocatalytic approaches are important developments, they still suffer from the same drawback as the synthetic methods in requiring stoichiometric amounts of toxic and potentially explosive diazo-carbene substrates as methylene donors, that are undesirable at industrial-scale. Thus, in this work we decided to investigate alternative biocatalytic cyclopropanation approaches that operate under mild conditions and that are not diazo-carbene dependent.

Herein, we report the development of *E. coli* CFAS (*ec*CFAS) into a biocatalyst for the cyclopropanation of phospholipids and the enantioselective synthesis of methyl dihydrosterculate **1**. In doing so we have acquired new insight into this class of enzymes. Cyclopropane fatty acid synthases (CFAS) are a class of *S*-adenosylmethionine (SAM) dependent methyltransferase enzymes (MTases).[14] Unlike classic MTases which transfer a methyl group from SAM to a substrate, CFASs catalyse the cyclopropanation of unsaturated lipids in bacteria, plants and parasites.[15] *ec*CFAS was structurally characterised in 2018 (PDB 6BQC),[16] and it is thought to be important in bacteria for the long-term survival of non-growing cells and resistance to environmental stress.[17] Early studies on CFAS enzymes hypothesised that the enzymatic cyclopropanation reaction proceeds by transfer of the SAM methyl group to the double bond of an unsaturated phospholipid with formation of a carbocation intermediate, followed by a base-catalysed cyclisation to form the 3-membered ring.[15–16] Crystal structures of mycolic acid cyclopropane synthase (PDB1 KPI and 1KPH)[18] and *L. acidophilus* CFAS[19] (PDB 5Z9O) provide evidence for the carbocation mediated mechanism as tyrosine side chains in the active site provide carbocation stabilisation. Despite the key role that CFASs play in the biology, physiology and virulence of bacteria, little is still known about their substrate specificity, regio- and stereoselectivity.[16b] In addition, since CFAS enzymes require SAM as a methylene donor instead of diazo-carbene co-substrates, they have the potential to be mild and more sustainable cyclopropanation biocatalysts.

In this work we investigated, for the first time, the stereo- and regioselectivity of the *ec*CFAS catalysed cyclopropanation of phospholipids. Substrate screening, rational mutagenesis and *in silico* studies have revealed first insights into the relationship between catalysis and substrate properties, such as lipid head group and lipid macromolecular/supramolecular structure, that are crucial for developing the enzyme into a sustainable biocatalyst for cyclopropanation reactions. Finally, purified *ec*CFAS was used as a mild biocatalyst in the enantioselective synthesis of methyl dihydrosterculate **1**. The biotransformation was optimised by using a halide methyltransferase (HMT) to biocatalytically regenerate the expensive SAM cofactor with cheap CH_3I in an enzymatic cascade. Figure 1.

Results and Discussion

Production and methyltransferase activity of ecCFAS. Recombinant *E. coli* CFAS (accession number UHR05351.1) was expressed as an *N*-terminal His_6-tagged protein (*ec*CFAS) in *E. coli* T7 and purified via NTA chromatography. Size exclusion chromatography (SEC) confirmed the enzyme to be a homo-dimer in solution as previously reported[16a] (Figure S5). Purified recombinant *ec*CFAS was assayed for methyltransferase activity using a commercially available methyltransferase colourimetric assay (Figure 2a). As little data was available on the substrate selectivity of *ec*CFAS, the commercially available *E. coli* Polar Lipid Extract (PLE, Avanti Polar Lipids) (1 mM), composed of 18:1-Δ9-*cis*-phosphatidylglycerol (PG, 67%), 18:1-Δ9-*cis*-phosphatidylethanolamine (PE, 23.2%) and 18:2-Δ9-*cis*-cardiolipin (CL, 9.8%), was initially used to assay *ec*CFAS activity, at varying enzyme concentrations (0.03 μM to 1 μM), Figures 2b–c.[20] The enzyme was also assayed with several single lipids, PG, PE, phosphatidyl serine (PS), phosphatidyl choline (PC) and phosphatidic acid (PA) which present the same lipid chains (18:1-Δ9-*cis*) but different polar heads (Figure S19). The fully saturated synthetic phospholipid 1,2-dimyristoyl-*syn*-glycero-3-phosphocholine (PC 14:0), was used as negative control. The colourimetric assay works by indirectly monitoring the levels and consumption of the S-adenosyl methionine (SAM) co-factor present in the assay reactions which is responsible for the

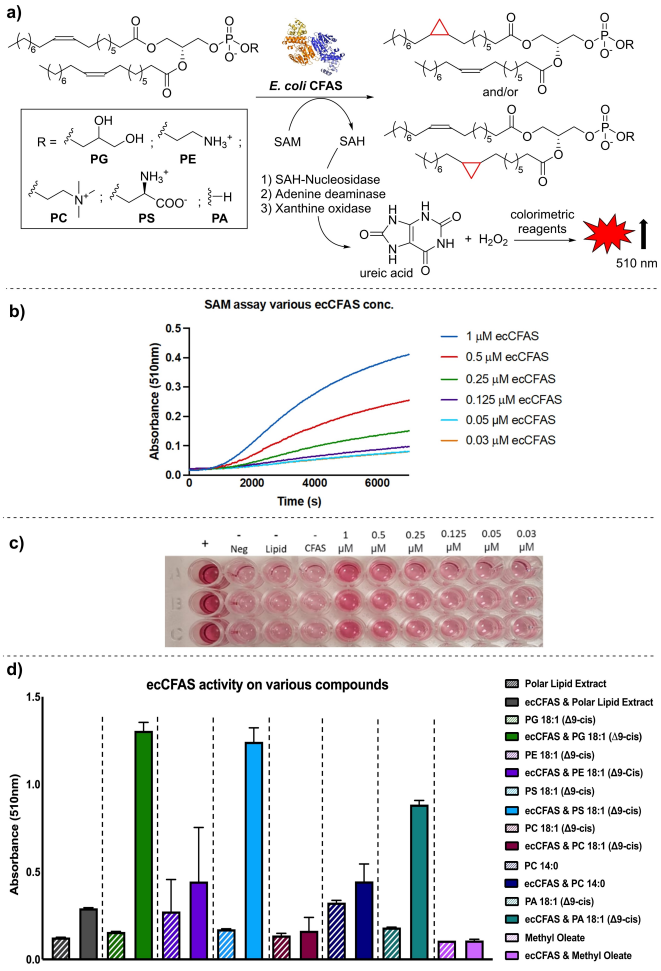

Figure 2. *ec*CFAS methyl transferase activity assay. [a] Scheme of the methyltransferase colourimetric assay. The activity of *ec*CFAS is determined indirectly through enzymatic decomposition of SAH; [b] Methyltransferase activity on *E. coli* Polar Lipid Extract (PLE) monitored overtime with increasing *ec*CFAS enzyme concentration (a constant polar lipid concentration of 1 mg/mL was used); [c] Representative image of the SAM assay (Merck Millipore, CBA096) showing the colourimetric change observed following each reaction. + = positive control reaction with SAH, – Neg = negative control reaction lacking both CFAS and the polar lipid extract, – CFAS = negative control reaction lacking CFAS, - Lipid = negative control sample lacking the polar lipid extract; [d] Maximum absorbance measured for different phospholipid substrates in presence (solid bars) or absence (hashed bars) of *ec*CFAS (1 μM), lipid (1 mM) after 3 h. PE 18:1 was co-solubilised with fully saturated PC 14:0 (PE18:1/PC14:0 ratio 4:1) to overcome the low PE solubility in buffer. All lipid structures are given in Figure S19. Data is presented as Mean ± SEM where $n = 3$. Based on the data in Figure 4, the lag phase is likely an artefact of this assay.

transfer of the methylene unit to the double bond of the phospholipids. All the 18:1-Δ9-*cis* phospholipids led to a positive colourimetric assay (Figures 2c–d), with PG being the preferred substrate. PC-14:0 does not contain a double bond and thus, as expected, no activity was detected. Finally, *ec*CFAS was assayed with oleic acid and methyl oleate, but no conversion was detected, suggesting that the presence of the phosphate polar head is important for substrate recognition. PG was thus chosen as a model substrate for subsequent studies.

Confirmation of ecCFAS cyclopropanation activity. The colourimetric assay provided only indirect confirmation of the *ec*CFAS methyltransferase activity on PG.

To confirm that *ec*CFAS was indeed cyclopropanating PG, the synthesis of methyl dihydrosterculate **1** was analysed via GC-MS (Table 1). *ec*CFAS was assayed with PG in the presence of SAM and recombinant SAH nucleosidase (SAH-N), used to degrade SAH, an *ec*CFAS inhibitor (K_i 220 μM), formed during the biotransformation.[16b] The biotransformations were carried out in HEPES buffer containing 150 mM $NaHCO_3$, as the base essential for the deprotonation of the carbocation intermediate and the cyclopropanation reaction.[15–16,21] The cyclopropanated phospholipid products were hydrolysed and derivatised for GC-MS analysis to produce the methyl dihydrosterculate **1**.

Methyldecanoate and a racemic synthetic standard of **1**, synthesised via Simmon-Smith reaction, were used as reference standards to calculate the conversion of the biocatalytic cyclopropanation (Table 1 and Table S7). The optimal concentration of *ec*CFAS enzyme was first investigated using PG at 4 mM concentration, 4 mM (1 eq) of SAM and SAH-N in equal concentration to *ec*CFAS. Comparable GC conversions of ester **1** (18 %, Table 1, *entries 2–3*) were observed at 5–10 μM *ecCFAS* concentration, while low conversion was obtained when 1 μM of the enzyme was used (< 5 %, Table 1, *entry 1*). Thus, 5 μM was selected for further experiments. When 2 mM PG and 2 mM (1 eq) SAM were used, ester **1** was obtained with 25 % GC conversion (Table 1, *entry 5*). Increasing or decreasing PG/SAM concentrations led to a slight decrease in conversion (Table 1, *entries 4* and *6*), while almost no reaction was observed at higher concentrations of PG (32–64 mM, Table S7 and Figure S17). Increasing the concentration of SAM to 4 mM (2 eq) (*entry 7*) resulted in a remarkable improvement in reaction conversions of **1** to 42 %.[22] No differences in conversions were observed in adding SAM portion-wise over 3 h (*entry 8*). Increasing the amount of SAM (8 eq or higher) or time (16 h) did not affect the biotransformation.

Effects of phospholipid supramolecular structure on ec*CFAS activity.* In all the above reactions, PG was suspended in buffer, likely forming vesicles and micelles. According to the proposed mechanism,[16] *ec*CFAS interacts with the phospholipid polar head groups of the bacterial membranes through the *N*-terminal domain, while the active site spans the *C*-domains of both monomers. Since *ec*CFAS in nature acts on bacterial membranes, we hypothesised that the size and curvature of the PG vesicles may affect the enzyme activity.

DLS was used to determine size distribution of the vesicles after manipulation. Small unilamellar PG vesicles (SUVs, < 100 nm) were prepared by sonication,[16b] while large unilamellar PG vesicles (LUVs, 100 nm–1 μm) were prepared by extrusion (Figure 3). It was found that sonication produced inconsistent data, and the process resulted in an heterogeneous mixture of differently sized vesicles. On the other hand, PG vesicles prepared through extrusion

Table 1: Biocatalytic cyclopropanation of PG and synthesis of methyl dihydrosterculate **1**.

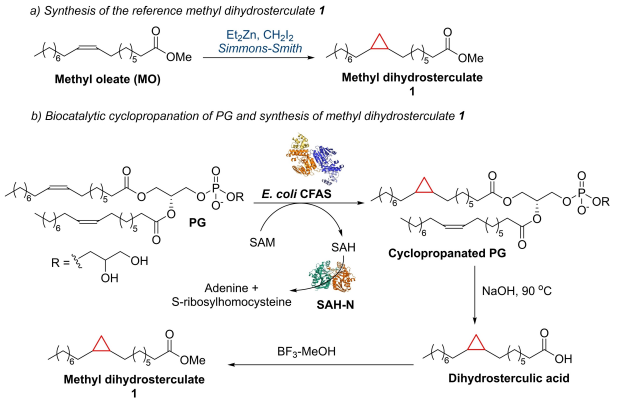

Entry	PG (mM)	CFAS (μM)	SAM (mM)	SAH–N (μM)	1 Conv. in 3 h (%)[a]	TON[b]
1	4	1	4 (1 eq)	1	<5	93
2	4	10	4 (1 eq)	10	17	135
3	4	5	4 (1 eq)	5	18	276
4	1	5	1 (1 eq)	5	18	74
5	2	5	2 (1 eq)	5	25	197
6	8	5	8 (1 eq)	5	12	368
7	2	5	4 (2 eq)	5	42 (43)[d]	338
8	2	5	2+2[c] (1+1 eq)	5	42	339
9	2	5	16 (8 eq)	5	41	324
10	2 (*son.*)[e]	5	4 (2 eq)	5	40–51	315
11	2 (ext.)[f]	5	4 (2 eq)	5	58	471

All the reactions were carried out for 3 h in HEPES buffer pH 7.5 at 37 °C; SAM eq are reported relative to PG. [a] GC-MS conversions were reported using methyldecanoate as internal standard; [b] TONs were calculated by means of a calibration curve of the chemically synthetized product dihydrosterculic acid methyl ester **1** (Figures S11–S12); TONs refer to conversion in 3 h; [c] 1 eq of SAM was added to the reaction mixture at t=0, and 1 eq of SAM was added after 1.5 h; [d] ^{1}H NMR conversion is reported in brackets; ^{1}H NMR analysis unambiguously confirmed the presence of a cyclopropane ring in **1** (Figure S18); [e] Sonicated PG was used (PG was sonicated for 30 min at room temperature before use); [f] Extruded PG was used (PG vesicles were prepared by extrusion to 100 nm before use).

were larger but with a consistent narrow size distribution (100–200 nm) (Figure 3b–c). Untreated PG forms larger vesicles with greater size distribution (250–600 nm). When sonicated PG (2 mM) was treated with *ec*CFAS (5 μM) and 4 mM SAM, the ester **1** was obtained with a variable 40–51 % GC yields (Table 1, *entry 10*). The variability in the yield is likely due to the heterogeneity in size and the strained conformations, due to curvature, of sonicated vesicles. Remarkably, the highest GC yield (58 %) was obtained from extruded PG (Table 1, *entry 11*), confirming the key role of the vesicle size, membrane curvature and homogeneity for the outcome of the biocatalytic reaction. It is evident that the supramolecular structure and size of the phospholipid vesicles affects substrate binding.

Stereo- and regioselectivity of the ecCFAS catalysed cyclopropanation of PG. Previous investigations of CFAS enzymes have provided only limited information on the enzyme's stereoselectivity.[23] The three-dimensional structure of the native cyclopropanated lipid PG is still unknown. This is a crucial piece of characterisation both for developing *ec*CFAS into a cyclopropanation biocatalyst and to understand the packing of cyclopropanated lipids in bacterial membranes. First, we assayed *ec*CFAS with 18:1-Δ9-*trans*-PG, bearing two *trans*-oleyl chains. Traces of cyclopropanated product were formed in the biotransformation, confirming that the *trans*-PG is not a substrate of *ec*CFAS and that the enzyme is selective for Δ9-*cis*-PG. Both the fatty acid chains of *cis*-PG contain a *Z* double bond at C9–C10, and the addition of a methylene unit from SAM to

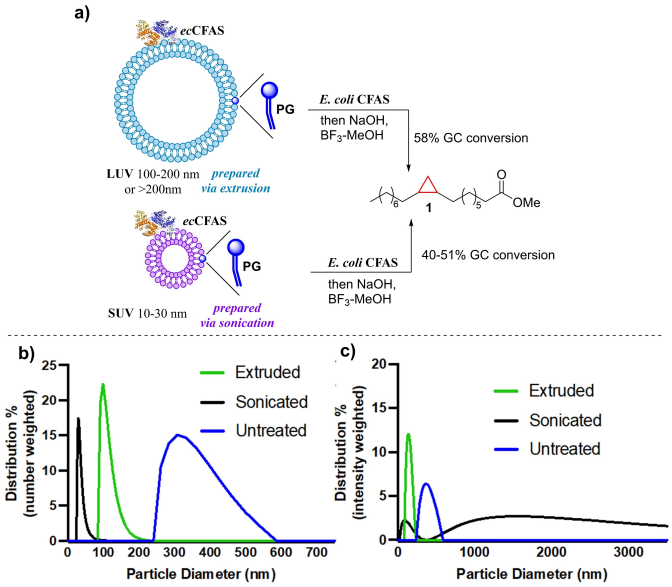

Figure 3. Size and distribution of PG vesicles. [a] Yields of **1** from cyclopropanation on LUV and SUV; Size distribution function of 100 mM untreated, sonicated and extruded PG in HEPES reaction buffer (pH 7.5) showing [b] the average/highest frequency liposome sizes and [c] the range of liposomes sizes.

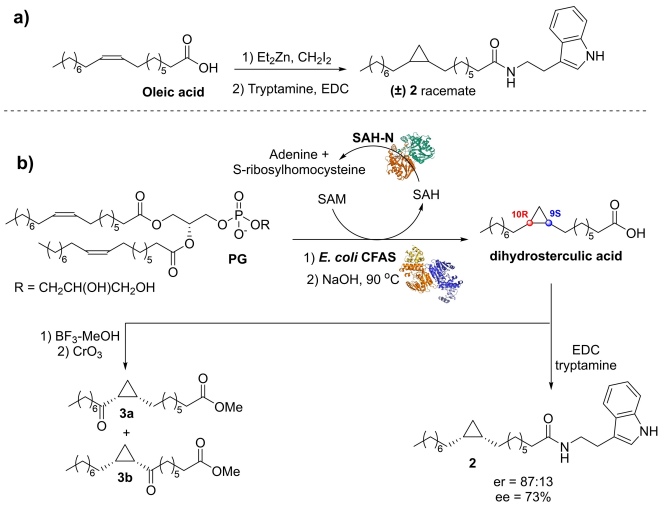

Scheme 1. Analysis and determination of the absolute configuration of dihydrosterculic acid obtained via *ec*CFAS cyclopropanation of PG. Accession numbers for all enzymes in the cascade can be found in Table S1.

the alkene moiety could lead to two possible cyclopropane enantiomers, (9*S*,10*R*)-PG and (9*R*, 10*S*)-PG. The stereoselectivity of the *ec*CFAS cyclopropanation of *cis*-PG was determined through HPLC analysis.

Racemic dihydrosterculic acid was derivatised with tryptamine to give racemic amide **2**. Enantiomers were separated by chiral HPLC (Figure S31) and compared with the corresponding derivatised products of the *ec*CFAS reaction with PG.

Chiral HPLC analysis of the biotransformation revealed that **2** was formed with 73 % ee. The absolute stereochemistry of cyclopropanated fatty acid derivatives was determined through comparison of the $[\alpha]_D$ values calculated for the oxidised derivatives **3a** and **3b** with the data reported in the literature (Scheme 1).[24] According to the observed $[\alpha]_D$ values, −11.9 for **3a** and +19.3 for **3b**, it was established that the absolute configuration of the dihydrosterculic acid (major enantiomer) and its derivatives was 9*S*,10*R*. The assigned configuration is in agreement with that of **1** isolated from *L. plantarum*, albeit with only 39 % ee,[25] while it is opposite to the configuration of **1** obtained from the plant *Litchi chinensis*,[24a] and to that of the quasienantiomer methyl lactobacillate (methyl (*Z*)-10-(2-hexylcyclopropane-1-yl)-decanoate) isolated from the lipid fraction of *E. coli* B-ATCC 11303.[23] The different observed configurations for quasienantiomers and enantiomers of **1** from different sources is intriguing, suggesting that different regioisomeric substrates of CFAS enzymes may lead to products with opposite configuration. We speculate that the flexibility of the PG chains may lead to multiple possible binding modes for the lipid chain in the active side, allowing the *Z*-alkene to attack the SAM from either face. Alternatively, one PG chain could be cyclopropanated resulting in one enantiomer and the other chain could produce the opposite configuration.

PG bears two unsaturated fatty chains which can be both or individually cyclopropanated by *ec*CFAS. Previous reports of CFAS activity, have not given any insight into regiochemistry of this transformation and on which acyl chain is cyclopropanated. This data is lost on phospholipid hydrolysis during derivatisation for GC-MS analysis. In principle, three possible phospholipid products could be formed in *ec*CFAS reactions, the mono-cyclopropanated (mono-CP) derivatives **4a** or **4b**, and the di-cyclopropanated (di-CP) phospholipid **4c** (Table 2). To retain regiochemical information, the *ec*CFAS biocatalysed cyclopropanation was investigated by LC–MS. When PG (2 mM) was reacted with *ec*CFAS under optimised conditions and analysed by LC–MS, we were surprised to see two products of different mass. The first corresponded to a mono-CP and the second corresponded to a di-CP product. To our knowledge, dicyclopropanation activity has not been previously reported for any CFAS enzyme. A 1:8 mono-CP/di-CP ratio of **4a–b**/**4c** was observed after 3 h (Figure 4a). Remarkably, the mono-CP/di-CP ratio *ec*CFAS dramatically changes when sonicated or extruded PG was used as substrate.

Sonicated PG provided an almost 1:1 ratio of **4a–b**/**4c**, while a 1:5 ratio of **4a–b**/**4c** was observed with extruded PG after 3 h, clearly indicating a relationship between the vesicle size, the vesicle curvature and the preference for mono- or di-cyclopropanation. A 1 h time point analysis of the cyclopropanation reaction revealed the rapid formation of mono-CP **4a–b** and di-CP **4c** in the first 5 min. (Figure 4b). After such time, the mono-CP **4a–b** intermediate is slowly almost fully converted to di-CP **4c**, remarkably indicating the unexpected preference of *ec*CFAS for the cyclopropanated substrate. After 1 h, almost 50 % of the PG is cyclopropanated.

Table 2: Structure of the possible cyclopropanated products **4a**, **4b** and **4c** and effects of SAM concentration on the unreacted, mono-CP and di-CP products ratio.

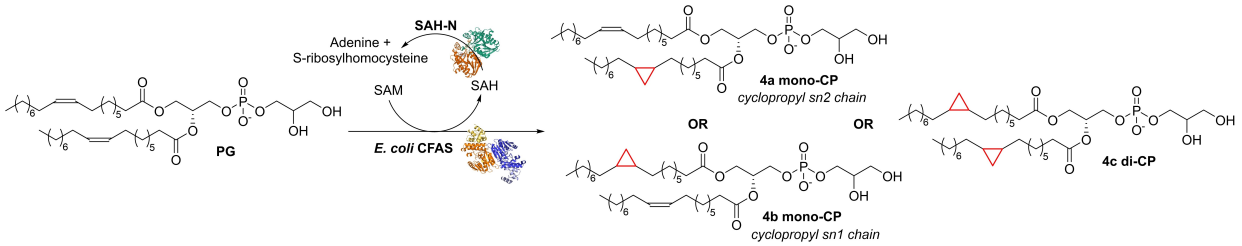

Entry	PG (extruded)	*ec*CFAS μM	SAM mM (eq)	SAH-N μM	Unreacted PG %	Mono-CP 4a-b %	Di-CP 4c %	di-CP/mono-CP ratio
1	2 mM	5	4 (2 eq)	5	36	11	52	4.9
2	2 mM	5	2 (1 eq)	5	47	26	27	1.01
3	2 mM	5	2+2 (1+1 eq)	5	36	15	49	3.3
4	2 mM	5	8 (4 eq)	5	37	8	55	6.8
5	2 mM	5	16 (8 eq)	5	34	6	60	10
6	2 mM	1	4 (2 eq)	5	55	23	22	0.95
7	2 mM	2	4 (2 eq)	5	44	18	38	2.1
8	2 mM	10	4 (2 eq)	10	31	7	62	8.8

% of unreacted-PG, mono-CP and di-CP was measured by LC–MS and presented as the average % of 3 repeats.

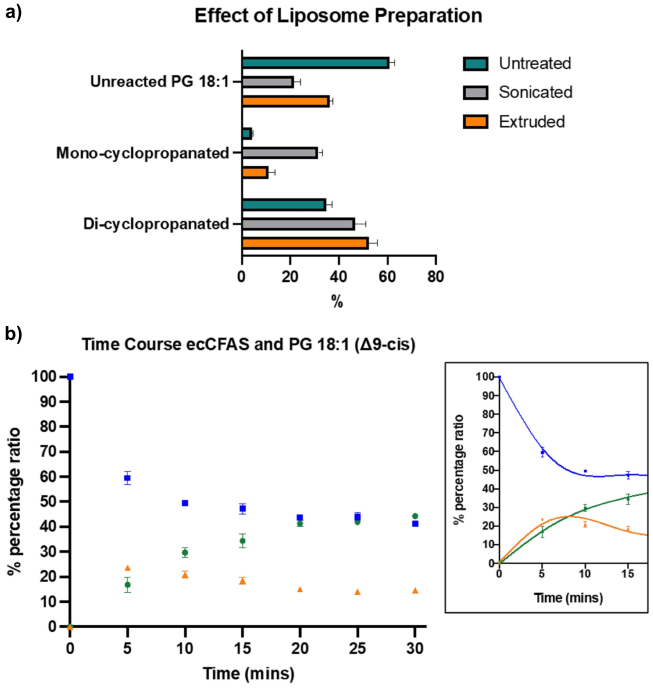

Figure 4. Regioselectivity of *ec*CFAS enzymatic cyclopropanation of PG. [a] Ratio of unreacted, mono-CP and di-CP products from untreated, sonicated and extruded PG. All the reactions were run for 3 h; [b] Time course of the enzymatic cyclopropanation of extruded PG showing the different rate of formation of mono-CP and di-CP products. Reaction conditions: 2 mM extruded PG, 5 μM *ec*CFAS, 5 μM SAH-N, 4 mM SAM, 37 °C, 1 h. Data is presented as Mean ± SEM where $n = 3$.

This data demonstrates that *ec*CFAS cyclopropanates one acyl chain, this product is released, and is preferentially rebound such that the other non-cyclopropanated acyl chain now sits in the active site. Interestingly, the concentration of SAM and *ec*CFAS also affected the mono-CP/di-CP ratio of the biocatalytic transformation (Table 2).[26] When 1 eq of SAM was used an almost 1:1 di-CP/ mono-CP ratio was observed (Table 2, *entry 2*). The ratio increases as more equivalents of SAM are used, showing a clear linear correlation between the amount of SAM in the biocatalytic transformation and the formation of the di-cyclopropanated product **4c** (Table 2, *entries 1 and 3–5*). A similar trend was observed when the concentration of *ec*CFAS was increased from 1 μM to 10 μM (Table 2, *entries 6–8*). *In-silico* docking studies suggest that the *sn1* chain preferentially binds the *C*-terminal catalytic site over the *sn2* chain (Figure 6a and Table S2).

Activity of ec*CFAS on various phospholipids lipids.* Surprisingly, given the range of lipids present in bacterial membranes there is little information on the substrate specificity of *ec*CFAS.[16b] Our initial colourimetric methyltransferase activity assay indicates that, while *ec*CFAS has a preference for PG, it is capable of accepting multiple substrates. With a robust and direct LC–MS method we could understand if the ratio of the mono- and di-cyclopropanated lipids was the same across all substrates. Our data (Figure 5a) indicates that in terms of conversion, the preferred substrate of *ec*CFAS is PG (54 %) followed by PS (45 %), then PE (24 %). As all chain lengths and double bond positions are the same, this indicates a clear preference of *ec*CFAS for neutral or zwitterionic phospholipid headgroups. In fact, the positively charged PE and negatively charged PA were poor substrates.[27] Additionally, PC proved to not be a substrate of *ec*CFAS, likely due to the increased steric bulkiness on the phospholipid amine headgroup. However, electronic rather than steric appear to be the major contributory factors dictating the phospholipid and headgroup preference. The second notable result from this substrate screen is the product distribution. Unexpectedly, while di-cyclopropanated products are formed in all cases, the mono-cyclopropanated product dominates for all

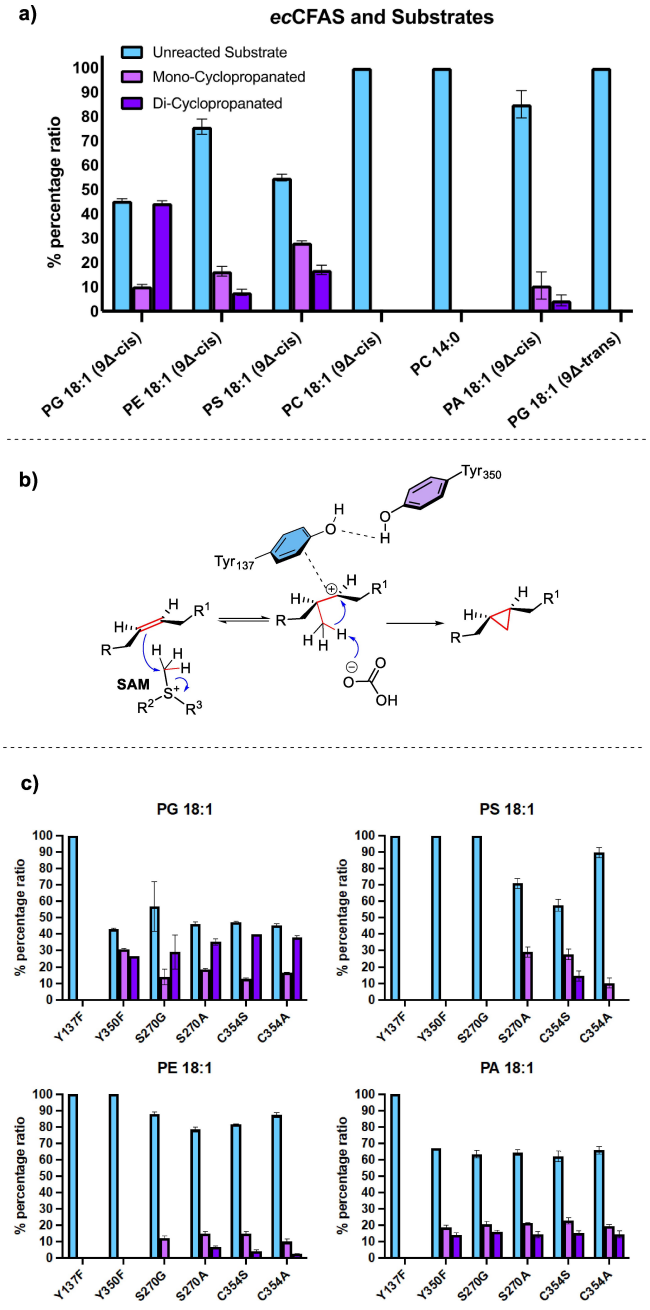

Figure 5. [a] Activity of *ec*CFAS on different phospholipids and mono-CP/di-CP products ratio. All the reactions were carried out with 5 μM *ec*CFAS, 5 μM SAH–N, phospholipid 2 mM, SAM 4 mM in 100 mM HEPES buffer pH 7.5, 150 mM $NaHCO_3$, 37 °C, 300 rpm, 100 μL reaction volume. Lipids were prepared by extrusion to 100 nm. PE 18:1 was co-solubilised with PC 14:0 (PE18:1/PC14:0 4:1) to overcome the low PE solubility in buffer; [b] Proposed mechanism for *ec*CFAS showing the role of the Tyr137 and Tyr350 residues; [c] Evaluation of mutants on PG, PS, PE and PA. Data is presented as Mean ± SEM where $n = 3$.

substrates, except for PG. This indicates a lower affinity of *ec*CFAS for other mono-cyclopropanated lipids compared to **4a**/**4b**. An in silico *ec*CFAS model (Figure S39a) containing the SAM cofactor was built using the available crystal structure of *ec*CFAS co-crystallised with the carbonate ion and a lipid ligand (PDB ID: 6BQC),[16a] and CFAS from *Aquifex aeolicous*, co-crystallised with SAM (sequence identity 36 %; PDB ID: 7QOS).[28] According to the currently accepted cyclopropanation mechanism, CFAS enzymes catalyse the cyclopropanation of phospholipids via a carbocation intermediate where the Tyr137 hydroxyl group actively stabilises the transient positive charge (Figure 5b). A key role in the catalytic mechanism seems also to be played by Tyr350 which increases the stabilising effect of Tyr137 through a hydrogen bond interaction.[16a,29] Multiple sequence alignments of *ec*CFAS with other bacterial CFAS proteins[18,19] highlights that these two residues are highly conserved across bacterial species. PG and PS place their phospholipid headgroups in the *N*-terminal region of *ec*CFAS forming specific interactions with the surrounding residues (Figures 6a and S39b).

PE presents an optimal disposition of the phospholipid headgroup and interactions with residues Asp274 and Asn276; however, the high solvent exposure of one of PE's chains indicates a less stable occupation of the active site, which is reflected in the observed reduced cyclopropanation (Figure S39c).

PC also assumes a non-ideal conformation to maintain the Δ9-*cis* double bond chain in proximity of Tyr137, placing the headgroup in a different region of the protein and completely exposing the second chain to the solvent (Figure S40a). Such data confirms the unsuitability of PC as *ec*CFAS substrate.

To investigate the role of Tyr137 and Tyr350 in *ec*CFAS catalysis, two mutants *ec*CFAS_Y137F[21] and *ec*CFAS_Y350F, were generated and their activity screened with phospholipid substrates (Figure 5c). Mutation of Tyr137 to Phe completely abolished any catalytic activity on all phospholipids, thus Tyr137 appears crucial for catalysis, presumably by stabilising the carbocation intermediate (Figure 5b). However, computational studies indicate that Tyr137 also has a substrate binding role as data clearly shows that PG, PS and PE are unable to bind to *ec*CFAS_Y137F in an ideal conformation with the double bond exposed to SAM (Figures 6b and S40b). These findings suggest that Tyr137, as well as having a crucial role in stabilising the carbocation intermediate, may have a structural role in maintaining the correct architecture of the catalytic site. Unexpectedly, mutation of Tyr350 to Phe changed the substrate specificity of *ec*CFAS. The mutant enzyme is still able to cyclopropanate PG with comparable conversion to the WT enzyme, although the di-CP/mono-CP ratio changed so that less di-CP is produced indicating a reduced affinity of the mutant for the mono-CP lipid (Figure 5). The mutant also showed a similar activity to that of the WT with PA with no significant impact on di-CP/mono-CP ratio. Surprisingly, this quite conservative mutation abolished activity on PE and PS. As the chains of the phospholipids are identical, this intriguing mutation appears to affect, not the catalytic activity, but the ability of the enzyme to recognise the substrate, likely via an allosteric effect. Tyr350 is in a helix linked to a loop around the head group. Mutation could alter the orientation of the positively charged residues like Lys271 and Lys272 resulting in

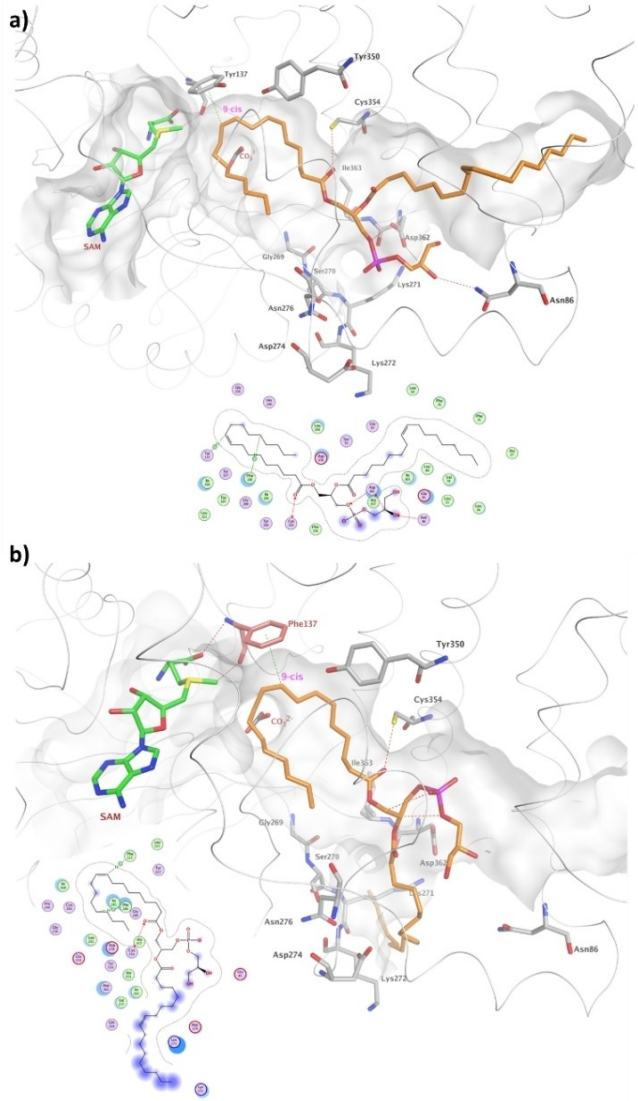

Figure 6. [a] Proposed binding modes for PG in WT *ec*CFAS; [b] Proposed binding modes for PG in mutant Y137F. Carbon atoms of PG are shown in orange. The binding area of the catalytic site is represented as a transparent grey surface. Carbon atoms of SAM cofactor are shown in green. The *ec*CFAS is shown as thin ribbon. H-bonds are shown as red dots, whereas hydrophobic interactions are represented as green dots. The mutated residue is coloured and labelled in red. Blue shadow areas on the 2D molecule-enzyme interactions diagram represent solvent exposure areas.

repulsion of the ethanolamine headgroup. Such hypotheses were supported by docking analysis. Whilst the Y350F mutation does not influence the binding mode of PG, which is still able to correctly occupy the active site, no docking outputs or stable binding modes were obtained for PS and PE (Figures S37a and S40c). The results of investigations into Y350F led us to investigate Ser270 which is in the head group binding region and forms hydrogen bonds to the lipid phosphate group and, intriguingly, the amide backbones of both Lys 271 and Lys272.

Mutants S270A and S270G were created to remove the hydrogen bonding and increase loop flexibility respectively. Excitingly, both mutants impacted the same substrates as Y350F, albeit to a lesser degree. However, S270G has the greatest impact on substrate selectivity introducing increased flexibility. This indicates a clear relationship between this helix and loop region and substrate recognition. The S270G mutation keeps unmodified PG and PE binding (Figures S37b and S41a), whereas PS loses an important anchoring point to the enzyme, causing the headgroup to move away exposing the phospholipid to the solvent (Figure S40b). On the other hand, PS is still able to properly occupy the binding site of the S270 A mutant placing its headgroup and the lateral chain in the correct areas of the active site (Figure S38). Finally, Cys354 is indicated in the *ec*CFAS crystal structure as interacting with the lipid acyl chain carbonyl oxygen. C354S and C345A mutants however showed little change from the wild-type indicating that this is not a crucial interaction for substrate binding or recognition. Unsurprisingly, none of the mutants conferred activity on PC substrates.

SAM regeneration using halide methyltransferase (HMT). Finally, having generated new insights into *ec*CFAS catalysed cyclopropanation, we began to investigate methods to exploit the enzyme as a biocatalyst for cyclopropanation reactions. A limitation of methyltransferase enzymes in biocatalysis is the need for expensive and unstable SAM cofactor as methyl donor. To exploit *ec*CFAS as biocatalyst, we explored a SAM regeneration system. Halide methyltransferases (HMTs) have been reported to catalyse the synthesis of SAM from SAH in the presence of CH_3I and they have been used in many MTase biocatalysed transformations.[30–32] Untreated PG was reacted with *ec*CFAS (5 μM) in the presence of 2 mM PG, 10 μM HMT from *Arabidopsis thaliana* (*At*HMT)[33] and an excess of CH_3I (10 mM) and varying SAM concentrations. The formation of ester **1** was monitored by GC-MS. All reactions were initially carried out at 27 °C, the optimal temperature at which *At*HMT operates. However, 30 °C was found to be optimal for the cascade (Table S11). Remarkably, in all cases where <1 mM SAM was used, the cyclopropyl derivative **1** was obtained with good GC conversions (46–52 %, Table 3, *entries 1–3*) similar to those observed in the reactions with stoichiometric SAM. The conversions observed in the 0.2–1 mM SAM concentration range (*entries 1–3*) are consistent with the observed kinetic constants of the enzyme for SAM and pure PG substrate (Figure S27). Remarkably, we could replicate the conversion of **1** (50 %) obtained using stoichiometric SAM, by instead using *At*HMT and just 0.2 mM (0.1 eq) SAM (Table 3, *entry 3*). Negative controls (Table S11) confirmed the role of *At*HMT in the regeneration of SAM.[34] The use of extruded instead of untreated PG did not improve conversion (Table 3, *entry 4*). Conversion was however improved (64 %) by lowering the concentration of CH_3I (5 mM) (Table 3, *entry 6*). Finally, by changing CH_3I to CD_3I we generated deuterated lipid products in a quick and facile process. Deuterated lipids and fatty acids have shown their ability to reduce oxidative stress in cells and to be potentially useful in the treatment of neurodegenerative diseases and aging processes.[35] Using the optimised conditions for the cascade,

Table 3: Biocatalytic synthesis of methyl dihydrosterculate **1** using *ec*CFAS and catalytic SAM.

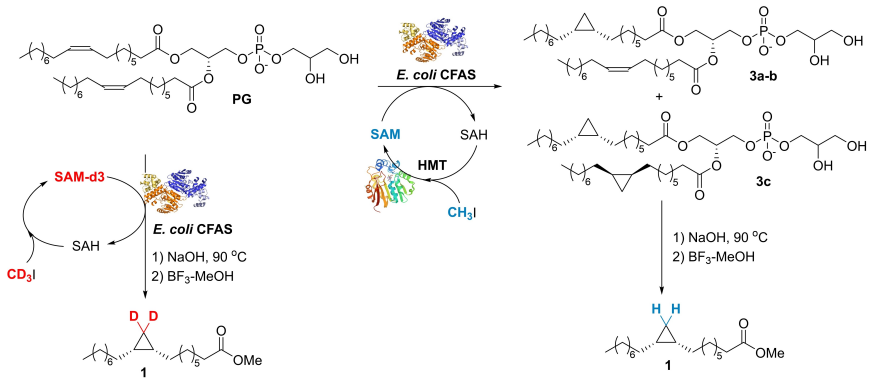

Entry	PG (mM)	ecCFAS (μM)	SAM mM (eq)	HMT (μM)	MeI (mM)	Temp. (°C)	Ester 1 GC-MS Conv. %[a]
1	2	5	1 (0.5)	10	10	27	46
2	2	5	0.5 (0.25)	10	10	27	52
3	2	5	0.2 (0.1)	10	10	27	50 (45)[b,c]
4	2 (ext.)	5	0.2 (0.1)	10	10	27	44
5	2 (ext.)	5	0.2 (0.1)	5	10	30	42
6	2 (ext.)	5	0.2 (0.1)	10	5	30	64
7[d]	2 (ext.)	5	0.2 (0.1)	10	5[d]	30	70

[a] GC-MS conversions are reported. Dihydrosterculic acid methyl ester **1** was used as reference; [b] ^{1}H NMR conversion is reported in brackets (see also Fig S18); [c] Methyl dihydrosterculate **1** was obtained with 67% ee as determined by HPLC analysis after appropriate derivatisation into **2**. [d] CD_3I was used as methylating agent. Accession numbers for all enzymes in the casecade can be found in Table S1.

the deuterated cyclopropane derivative **1** was synthesised with very high conversion using CD_3I (Table 3, *entry 7*).

Conclusion

In conclusion, the product profile, stereoselectivity and substrate specificity of *E. coli* CFAS in catalysing the cyclopropanation of various phospholipids has been demonstrated. PG (18:1-Δ9-cis) was found to be the preferred substrate of *ec*CFAS, and to be cyclopropanated at both lipid chains. To our knowledge this represents the first report of dicyclopropanation by CFAS enzymes. *ec*CFAS showed cyclopropanation activity also on other 18:1-Δ9-*cis* phospholipids, namely PS, PE and PA, while no activity was observed on 18:1-Δ9-*cis* PC and 18:1-Δ9-*trans* PG. Remarkably, this work shows, for the first time, the correlation between the activity of *ec*CFAS and the phospholipids supramolecular structure. The amount of cyclopropanated phospholipid formed in the enzymatic reactions varies depending on whether the phospholipid substrate is in the form of SUV, LUV or random lipid aggregates, with the best conversions and TON observed with LUV. The concentration of the SAM cofactor and the enzyme itself also affect the *ec*CFAS activity as well as the formation of mono-cyclopropanated or di-cyclopropanated phospholipid products as showed by LC–MS analysis. The preference for mono- versus di-cyclopropanation is affected by the nature of the phospholipid substrate and it seems correlated to the electronic properties of their headgroups, with higher conversions observed with neutral and zwitterionic head groups. Mutagenesis and *in silico* experiments were carried out to confirm the role of several amino acids involved in the catalytic cyclopropanation. The amino acid Tyr137 is shown to be essential for the activity of *ec*CFAS. Importantly, via mutation of Tyr350 and Ser270 we have identified key structural motifs which control substrate selectivity directly or intriguingly, via allosteric change. Indeed, Tyr350 and Ser270 are important to allow *ec*CFAS to act on a range of lipids with varying headgroups. For the first time, we also disclose the stereoselectivity of *ec*CFAS, showing that the enzyme catalyses the cyclopropanation of the PG fatty chains with a high degree of selectivity. The derivative methyl dihydrosterculate **1**, arising from the derivatisation of the cyclopropanated PG, was obtained with 73% ee and the absolute configuration was determined. Finally, a catalytic system for the synthesis of methyl dihydrosterculate **1** was developed combining purified *ec*CFAS with *At*HMT, allowing the cyclopropanation of PG to occur in the presence of a catalytic amount of SAM cofactor. This work demonstrates the potential of CFAS enzymes as biocatalysts for carbene free cyclopropanation reactions. Whilst this methodology provided a green route to the synthesis of cyclopropanated lipids, significant additional work is required to enable the use of CFAS enzymes as biocatalysts for the cyclopropanation of non-lipid substrates.

Supporting Information

Preparation of the enzymes, biology and biocatalytic procedures, synthetic procedures, copies of NMR and MS spectra, compounds characterisation.

Acknowledgements

We gratefully acknowledge BBSRC LIDo (BB/M009513/1) for PhD Studentships to IO, China Scholarship Council (CSC, scholarship No 202108310078) for PhD studentship to CL, GlaxoSmithKline Research and Development Ltd (BIDS3000037082) for PhD Studentship to BC, UCL for studentship to KP. For MC and DC this project has received funding from the European Union's Horizon 2020 research and innovation programme under the Marie Skłodowska-Curie (grant agreement n° 101027045). BBSRC-BIOCATNET (POC-045, R116824) is acknowledged for financial support to DC. BBSRC (BB/P019811/1) is acknowledged for funding to SMB. For AvN and CEP this project has received funding from the European Research Council (ERC) under the European Union's Horizon 2020 research and innovation programme (grant agreement n° 949910). Dr Heather Findlay is gratefully acknowledged for help with lipid preparation.

Conflict of Interest

The authors declare no conflict of interest.

Keywords: Biocatalysis · Cyclopropane · Enzymes · Methyltransferases · S-Adenosyl methionine regeneration

[1] a) M. Yasumoto, K. Mada, T. Ooi, T. Kusumi, *J. Nat. Prod.* **2000**, *63*, 1534–1536; b) Y.-Y. Fan, X.-H. Gao, J.-M. Yue, *Sci. China Chem.* **2016**, *59*, 1126–1141; c) W. Donaldson, *Tetrahedron.* **2001**, *57*, 8589–8627.
[2] D. Poger, A. E. Mark, *J. Phys. Chem. B.* **2015**, *119*, 5487–5495.
[3] N. M. Aston, P. Bamborough, J. B. Buckton, C. D. Edwards, D. S. Holmes, K. L. Jones, V. K. Patel, P. A. Smee, D. O. Somers, G. Vitulli, A. L. Walker, *J. Med. Chem.* **2009**, *52*, 6257–6269.
[4] S. Ulrich, R. Ricken, P. Buspavanich, P. Schlattmann, M. Adli, *J. Clin. Psychopharmacol.* **2020**, *40*, 63–74.
[5] F. Micheli, P. Cavanni, D. Andreotti, R. Arban, R. Benedetti, B. Bertani, M. Bettati, L. Bettelini, G. Bonanomi, S. Braggio, R. Carletti, A. Checchia, M. Corsi, E. Fazzolari, S. Fontana, C. Marchioro, E. Merlo-Pich, M. Negri, B. Oliosi, E. Ratti, K. D. Read, M. Roscic, I. Sartori, S. Spada, G. Tedesco, L. Tarsi, S. Terreni, F. Visentini, A. Zocchi, L. Zonzini, R. Di Fabio, *J. Med. Chem.* **2010**, *53*, 4989–5001.
[6] a) T. T. Talele, *J. Med. Chem.* **2016**, *59*, 8712–8756; b) S. J. Chawner, M. J. Cases-Thomas, J. A. Bull, *Eur. J. Org. Chem.* **2017**, *34*, 5015–5024; c) J. Salaün, *Topics in Current Chemistry*, Vol. 207© Springer-Verlag Berlin Heidelberg **2000**.
[7] a) H. Lebel, J.-F. Marcoux, C. Molinaro, A. B. Charette, *Chem. Rev.* **2003**, *103*, 977–1050; b) H. M. L. Davies, R. E. J. Beckwith, *Chem. Rev.* **2003**, *103*, 2861–2904; c) A–H. Li, L. X. Dai, V. K. Aggarwal, *Chem. Rev.* **1997**, *97*, 2341–2372.
[8] a) C. Ebner, E. M. Carreira, *Chem. Rev.* **2017**, *117*, 11651–11679; b) D. Qianand, J. Zhang, *Chem. Rev.* **2015**, *44*, 677–698; c) W. Wu, Z. Ling, H. Jiang, *Org. Biomol. Chem.* **2018**, *16*, 7315–7329; d) E. Sansinenea, A. Ortiz, *Eur. J. Org. Chem.* **2022**, *33*, e202200210.
[9] H. E. Simmons, R. D. Smith, *J. Am. Chem. Soc.* **1959**, *81*, 4256–4264.
[10] E. J. Corey, M. Chaykovsky, *J. Am. Chem. Soc.* **1965**, *87*, 1353–1364.
[11] P. S. Coelho, E. M. Brustad, A. Kannan, F. H. Arnold, *Science* **2013**, *339*, 307–310.
[12] a) P. Bajaj, G. Sreenilayam, V. Tyagi, R. Fasan, *Angew. Chem. Int. Ed.* **2016**, *55*, 16110–16114; b) A. Tinoco, V. Steck, V. Tyagi, R. Fasan, *J. Am. Chem. Soc.* **2017**, *139*, 5293–5296.
[13] S. Wallace, E. P. Balskus, *Angew. Chem. Int. Ed.* **2015**, *54*, 7106–7109.
[14] A. E. Chung, J. H. Law, *Biochemistry* **1964**, *3*, 967–974.
[15] a) J. E. Cronan, T. Luk, *Microbiol. Mol. Biol. Rev.* **2022**, *86*, e00013–22; b) D. F. Iwig, A. Uchida, J. A. Stromberg, S. J. Booker, *J. Am. Chem. Soc.* **2005**, *127*, 11612–11613; c) D. F. Iwig, A. T. Grippe, T. A. McIntyre, S. J. Booker, *Biochemistry* **2004**, *43*, 13510–13524.
[16] a) S. B. Hari, R. A. Grant, R. T. Sauer, *Structure.* **2018**, *26*, 1251–1258; b) F. R. Taylor, J. E. Cronan, *Biochemistry* **1979**, *18*, 3292–3300; c) F. Courtois, C. Guérard, X. Thomas, O. Ploux, *Eur. J. Biochem.* **2004**, *271*, 4769–4778.
[17] a) L. Shabala, T. Ross, *Res. Microbiol.* **2008**, *159*, 458–461; b) Y.-Y. Cronan, J. E. Chang, *Mol. Microbiol.* **1999**, *33*, 249–259.
[18] C. C. Huang, C. V. Smith, M. S. Glickman, W. R. Jacobs Jr., J. C. Sacchettini, *J. Biol. Chem.* **2002**, *277*, 11559–11569.
[19] Y. Ma, C. Pan, Q. Wang, *J. Biochem.* **2019**, *166*, 139–147.
[20] K. M. Dorgan, W. L. Wooderchak, D. P. Wynn, E. L. Karschner, J. F. Alfaro, Y. Cui, Z. S. Zhou, J. M. Hevel, *Anal. Biochem.* **2006**, *350*, 249–255.
[21] F. Courtois, O. Ploux, *Biochemistry* **2005**, *44*, 13583–13590.
[22] No side products were formed from the *ec*CFAS biocatalysed transformation. Unreacted methyl oleate in 58 % yield was observed by GC-MS.
[23] L. J. Stuart, J. P. Buck, A. E. Tremblay, P. H. Buist, *Org. Lett.* **2006**, *8*, 79–81.
[24] a) L. J. Stuart, P. H. Buist, *Tetrahedron: Asymmetry* **2004**, *15*, 401–403; b) S. Shah, J. M. White, S. J. Williams, *Org. Biomol. Chem.* **2014**, *12*, 9427–9438; c) J. W. Palko, P. H. Buist, J. M. Manthorpe, *Tetrahedron: Asymmetry.* **2013**, *24*, 165–168.
[25] S. Rasonyi, Der sterische Verlauf der Cyclopropanringbildung in der Biosynthese der Dihydrosterculinsäure in *Lactobacillus plantarum.* Diss. ETH # 11318,1995.
[26] The slightly different conversion values observed between the GC-MS and LC–MS are ascribable to the methods used. In case of GC-MS method, the methyl dihydrosterculate was analysed after appropriate derivatisation of the phospholipids, while in case of LC–MS the crude phospholipids were directly injected in the instrument and analysed, making the latter a more direct method of analysis.
[27] PE was mixed with PC 14:0 (4:1 ratio PE/PC) to increase the PE solubility. However, the low reactivity of PE might be also ascribable to its poor ability to readily form vesicles, being a non-lamellar lipid, thus preventing its interaction with *ec*CFAS; see references, a) I. M. Hafez, P. R. Cullis, *Adv. Drug Delivery Rev.* **2001**, *47*, 139–48; b) C. P. Tilcock, P. R. Cullis, *Ann. N. Y. Acad. Sci.* **1987**, *492*, 88–102.
[28] T. Lukk, J. E. Cronan, S. K. Nair. PDB ID: 7QOS **2021**. 10.2210/pdb7qos/pdb.
[29] H. Lin, *Bioorg. Chem.* **2011**, *39*, 161–170.
[30] C. Liao, F. P. Seebeck, *Nat. Catal.* **2019**, *2*, 696–701.
[31] Q. Tang, C. W. Grathwol, A. S. Aslan-Üzel, S. Wu, A. Link, I. V. Pavlidis, C. P. S. Badenhorst, U. T. Bornscheuer, *Angew. Chem. Int. Ed.* **2021**, *60*, 1524–1527.

[32] K. H. Schulke, F. Ospina, K. Hörnschemeyer, S. Gergel, S. C. Hammer, *ChemBioChem* **2021**, *23*, e202100632.
[33] Y. Nagatoshi, T. Nakamura, *Plant Biotechnol.* **2007**, *24*, 503–506.
[34] L. L. Bengel, B. Aberle, A.-N. Egler-Kemmerer, S. Kienzle, B. Hauer, S. C. Hammer, *Angew. Chem. Int. Ed.* **2021**, *60*, 5554–5560.
[35] C. Beaudoin-Chabot, L. Wang, A. V. Smarun, D. Vidović, M. S. Shchepinov, G. Thibault, *Front. Plant Physiol.* **2019**, *10*, 641.

Manuscript received: February 19, 2024
Accepted manuscript online: April 25, 2024
Version of record online: ■■, ■■

Research Articles

Biocatalysis

I. Omar, M. Crotti, C. Li, K. Pisak, B. Czemerys, S. Ferla, A. van Noord, C. E. Paul, K. Karu, C. Ozbalci, U. Eggert, R. Lloyd, S. M. Barry,* D. Castagnolo* _____ **e202403493**

Insights into *E. coli* Cyclopropane Fatty Acid Synthase (CFAS) Towards Enantioselective Carbene Free Biocatalytic Cyclopropanation.

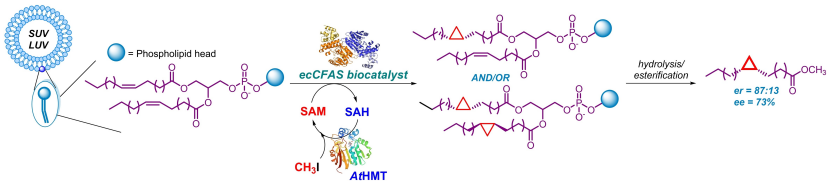

New insights into the stereo- and regioselectivity as well as catalytic activity of the *E. coli* CFAS enzyme are disclosed. The selectivity of *ec*CFAS in the cyclopropanation of various phospholipids and the influence of vesicle formation on the catalytic activity have been reported. Mutagenesis and in silico experiments have been carried out to identify the enzyme residues with key roles in catalysis. The biocatalytic synthesis of methyl dihydrosterculate was accomplished with *ec*CFAS and catalytic SAM cofactor.